Journal of Biomechanics ∎ (∎∎∎∎) ∎∎∎–∎∎∎

Contents lists available at ScienceDirect

Journal of Biomechanics

journal homepage: www.elsevier.com/locate/jbiomech
www.JBiomech.com

Ultrasound strain mapping of Achilles tendon compressive strain patterns during dorsiflexion

Ruth L. Chimenti [a,*], A. Samuel Flemister [b], John Ketz [b], Mary Bucklin [c], Mark R. Buckley [c], Michael S. Richards [d]

[a] University of Iowa, Department of Physical Therapy and Rehabilitation Science, United States
[b] University of Rochester, Department of Orthopaedic Surgery, United States
[c] University of Rochester, Department of Biomedical Engineering, United States
[d] University of Rochester, Department of Surgery, United States

ARTICLE INFO

Article history:
Accepted 11 November 2015

Keywords:
Ultrasound elastography
Achilles tendinopathy
Heel lift
Tendon strain

ABSTRACT

Heel lifts are commonly prescribed to patients with Achilles tendinopathy, yet little is known about the effect on tendon compressive strain. The purposes of the current study were to (1) develop a valid and reliable ultrasound elastography technique and algorithm to measure compressive strain of human Achilles tendon *in vivo*, (2) examine the effects of ankle dorsiflexion (lowering via controlled removal of a heel lift and partial squat) on compressive strain of the Achilles tendon insertion and (3) examine the relative compressive strain between the deep and superficial regions of the Achilles tendon insertion. All tasks started in a position equivalent to standing with a 30 mm heel lift. An ultrasound transducer positioned over the Achilles tendon insertion was used to capture radiofrequency images. A non-rigid image registration-based algorithm was used to estimate compressive strain of the tendon, which was divided into 2 regions (superficial, deep). The bland-Altman test and intraclass correlation coefficient were used to test validity and reliability. One-way repeated measures ANOVA was used to compare compressive strain between regions and across tasks. Compressive strain was accurately and reliably (ICC > 0.75) quantified. There was greater compressive strain during the combined task of lowering and partial squat compared to the lowering ($P=.001$) and partial squat ($P<.001$) tasks separately. There was greater compressive strain in the deep region of the tendon compared to the superficial for all tasks ($P=.001$). While these findings need to be examined in a pathological population, heel lifts may reduce tendon compressive strain during daily activities.

1. Introduction

Achilles tendinopathy affects approximately 6% of the general population during their lifetime (Kujala et al., 2005). One third of cases occur at the insertion (Fig. 1), known as insertional Achilles tendinopathy (IAT) (Karjalainen et al., 2000). A small wedge in the shoe, i.e. a heel lift, is often prescribed to relieve Achilles tendinopathy symptoms. Given that dorsiflexion requires tendon elongation, a heel lift positions the ankle in relative plantar flexion and thus reduces overall tendon strain (Farris et al., 2012). Additionally, heel lifts decrease plantar flexor muscle activity during walking (Akizuki et al., 2001; Johansoni et al., 2010; Lee et al., 1990), which reduces force on the tendon. Although there is limited evidence supporting its therapeutic use (Carcia et al., 2010; Scott et al., 2015), heel lifts are considered a component of standard care for Achilles tendinopathy.

Heel lifts may have an additional therapeutic role in the treatment of IAT by reducing calcaneal impingement. During dorsiflexion the posterior-superior surface of the calcaneus impinges against the deep side of the tendon insertion (Leitze et al., 2003; Shibuya et al., 2012) (Figs 1 and 2). This location of calcaneal impingement may contribute to IAT pathology, which is more prevalent on the deep side of the Achilles tendon (Karjalainen et al., 2000). Theoretically, an effect of common non-surgical (heel lifts) and surgical (resection of the posterior-superior calcaneal prominence) treatments for IAT may be a reduction of calcaneal impingement. However, to date there is no literature describing the magnitude or pattern of tendon compression during dorsiflexion, which could inform clinical theories on IAT treatment.

Ultrasound elastography is a quickly emerging technique that is effective at quantifying motion in a variety of human tissues (Athanasiou et al., 2010; Gennisson et al., 2010; Lopata et al., 2010; Muller

* Corresponding author. Tel.: +319 335 7149.
E-mail address: ruthchimenti@gmail.com (R.L. Chimenti).

http://dx.doi.org/10.1016/j.jbiomech.2015.11.008
0021-9290/

et al., 2009). In ultrasound elastography a sequence of images is collected as the tissue deforms. Select image pairs are compared to measure the deformation, i.e. tissue displacements, over the sequence of images. Strain maps can then be created from the resulting deformation measurements (Ophir et al., 1991). A limitation of ultrasound elastography is that the quality of the displacement, and subsequent strain, estimates decreases as tissue deformation increases (Cespedes and Ophir, 1997; Varghese, 1997). This is primarily due to an effect known as strain decorrelation, in which the image pair similarity is degraded by the relative motion of tissue features (e.g. acoustic scatterers) at a particular location (Kallel et al., 1997). Many researchers have published methods to compensate for strain decorrelation and improve the accuracy of strain estimates. A non-rigid image registration based strain estimator has been used in 3D static ultrasound elastography (Richards et al., 2009) and 2D intravascular ultrasound elastography (Richards and Doyley, 2013) to improve the quality of displacement and strain measures. Given that functionally the Achilles tendon experiences high strains, there is an inherent risk of strain decorrelation with *in vivo* measurements. Validation of an algorithm to process radiofrequency data is needed to test the accuracy of Achilles tendon strain estimates during activity.

Ultrasound elastography has been primarily utilized to quantify motion along the longitudinal axis of the tendon (Brown et al., 2013; Farris et al., 2012; Farron et al., 2009; Franz et al., 2015; Kim et al., 2011; Korstanje et al., 2012; Lichtwark and Wilson, 2006; Slane and Thelen, 2015; Yoshii et al., 2011). There is a lack of information on motion along the short axis of the tendon, which may have clinical implications for the treatment of insertional tendinopathies. In the current study, compressive strain is defined as the minimum principal strain. Due to the orientation of the maximum principal strain with the direction of tendon alignment (Fig. 3b), the compressive strain represents a coordinate system-independent measure of strain along the short axis of the tendon that is insensitive to probe positioning. The greater accuracy of quantifying compressive strain in parallel to the ultrasound beam, as opposed to tendon elongation perpendicular to the ultrasound beam (Lopata et al., 2009), affords the potential to accurately capture relatively large *in vivo* strains experienced by the Achilles tendon.

The purposes of the current study were to (1) develop a valid and reliable ultrasound elastography technique and algorithm to measure compressive strain of human Achilles tendon *in vivo*, (2) examine the effects of ankle dorsiflexion (lowering via controlled removal of a heel lift and partial squat) on compressive strain of the Achilles tendon insertion in healthy adults and (3) examine the relative compressive strain between the deep and superficial regions of the Achilles tendon insertion. The first hypothesis was that the algorithm used to analyze radiofrequency images would be a valid and reliable means of using ultrasound elastography to quantify tendon compressive strain. The second hypothesis was that ankle dorsiflexion would increase compressive strain. The third hypothesis was that there would be greater compressive strain in the deep region of the tendon compared to the superficial during dorsiflexion.

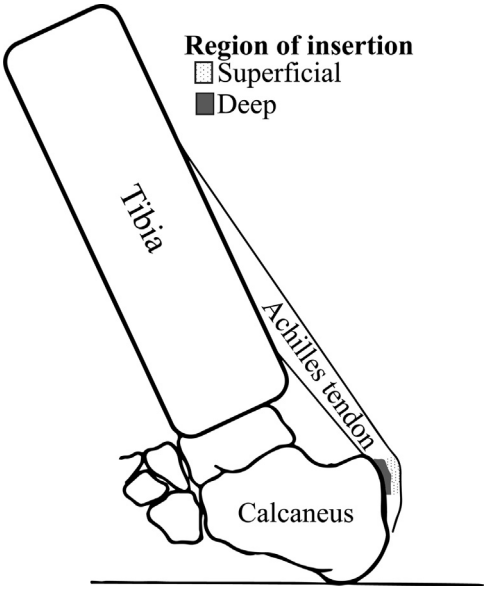

Fig. 1. During ankle dorsiflexion the posterior-superior prominence of the calcaneus impinges on the deep side of the Achilles tendon insertion.

2. Methods

2.1. Study participants

Ten adults (Sex: 4F/6M, Age: 35.7 ± 13.9 yrs, BMI: 24.1 ± 3.4 kg/m^2) without Achilles tendinopathy participated in the study. Participants were excluded if they had a condition that affected the Achilles tendon, including Achilles tendinopathy, rheumatological disease, diabetes, or history of ankle surgery. All subjects were informed of the study procedures and signed a consent form approved by the the University of Rochester's Research Subjects Review Board.

2.2. Experimental procedures

Tendon compressive strain was assessed during three weight-bearing tasks: (1) Lowering via a controlled removal of a heel lift, (2) Partial squat and (3) Lowering and partial squat (Fig. 2). All tasks started from the same position in standing with the heels at a 17° inclination relative to the toes, which is comparable to a 30 mm heel lift height. A pneumatic heel lift was built to passively lower the heels from a height of 30 mm (17° inclination) to a level surface. An inclinometer was used to achieve an equivalent inclination of the platform between tasks and participants. Air was released from the lift over a 3 s interval. Participants were instructed to perform a partial squat to their maximum tolerated ankle dorsiflexion over a time period of approximately 3 s, while maintaining their heels on the supporting surface. The

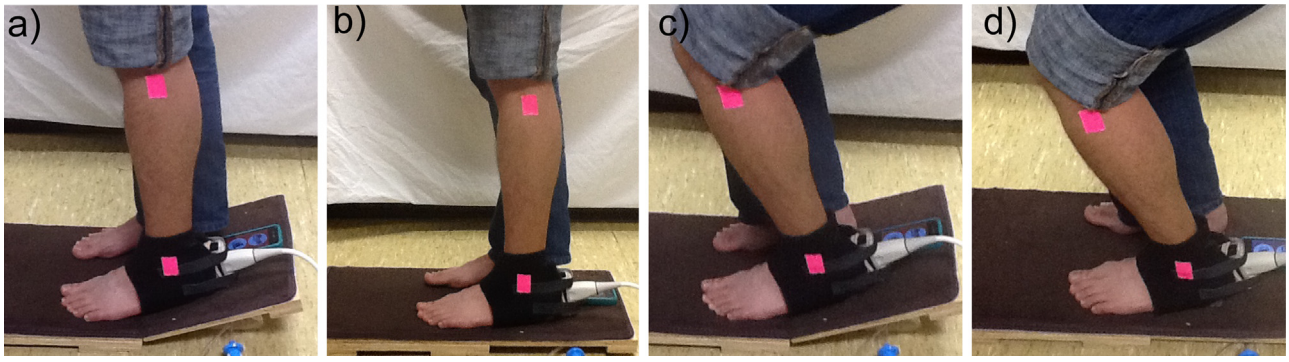

Fig. 2. All tasks were performed starting from the position shown in image a. The three tasks include: (1) Lowering (a)–(b), (2) Partial squat (a)–(c) and (3) Lowering and partial squat (a to b to c). The tape marks the position of the fibular head and lateral malleolus.

Please cite this article as: Chimenti, R.L., et al., Ultrasound strain mapping of Achilles tendon compressive strain patterns during dorsiflexion. Journal of Biomechanics (2015), http://dx.doi.org/10.1016/j.jbiomech.2015.11.008

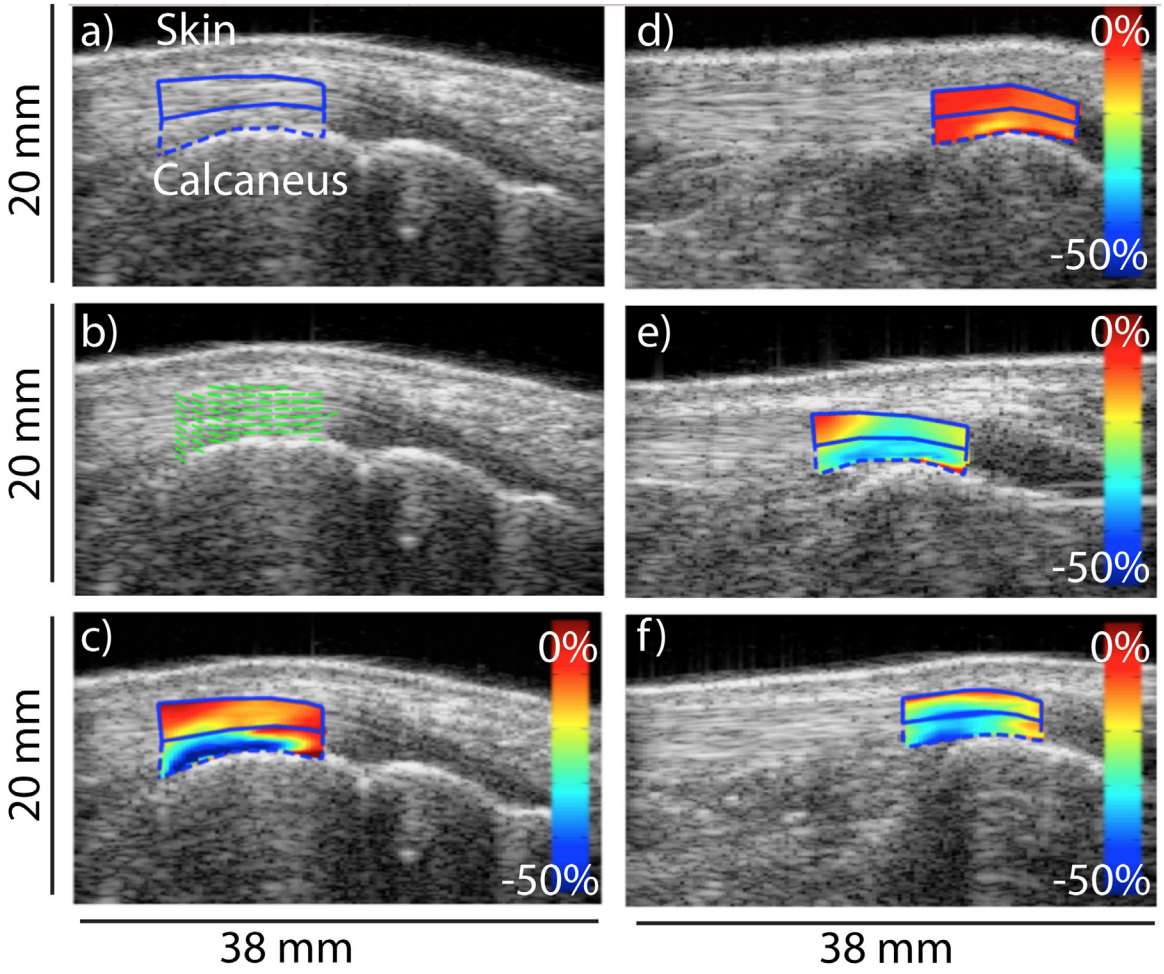

Fig. 3. Image series for one participant demonstrating (a) the regions of the Achilles tendon insertion with the superficial region outlined in solid blue line and the deep region in dashed blue line, (b) green lines represent the principal strain directions, (c) strain map during the combined task of lowering and partial squat and (d)–(f) range of strain maps in 3 different healthy adults during the combined task of lowering and partial squat . (For interpretation of the references to color in this figure, the reader is referred to the web version of this article)..

participants performed one practice trial of the partial squat, and then each task was repeated twice and the average was used as a representative trial.

Leg inclination was measured from videos recorded during each task. Reflective tape was placed on the fibular head and at the level of the lateral malleolus (Fig. 2). Leg inclination, as a function of time, was defined as the angle of the line between these two markers relative to the floor on each video frame. To capture Achilles tendon compressive strain an Ultrasonix, Sonix Touch Ultrasound system, capable of collecting the raw radiofrequency (RF) image data, and a linear array probe (L9-4/38) were used. The ultrasound images were collected with a center frequency of 10 MHz, a sampling frequency of 40 MHz, a depth of 3 cm and at a frame rate of 128 Hz. The ultrasound probe was stabilized by a custom 3D printed plastic shell, which was fixed to an ankle brace that had been modified by removing the fabric covering the tendon insertion (Fig. 2). An Aquaflex Ultrasound Gel Pad (Parker Laboratories, Fairfield, NJ) was used between the skin and the probe to improve contact and image quality.

To compare strains at equivalent leg inclinations for all subjects, the minimum principal strain was quantified at a leg inclination of 15°. This is similar to the amount of dorsiflexion needed to perform daily tasks such as walking and stair ascent (Andriacchi et al., 1980; Nester et al., 2014). Leg inclination measurements and ultrasound image data were visually inspected for the start and end of leg and calcaneal motion, respectively. Because the data was captured at different frame rates, the leg inclination was linearly interpolated to match the timing of the strain values.

2.3. Data analysis

Ultrasound strain measurements were calculated by first decimating in time the RF image frames, such that approximately 50 image frames spanned the time between the start and end of leg and calcaneal motion. A non-rigid image registration based strain estimator described previously (Richards et al., 2009; Richards and Doyley, 2013) was adapted to measure the total strain over the task. A 2D block matching, cross correlation based algorithm (Richards and Doyley, 2013) was used to obtain an initial estimate of the relative displacement fields for each successive frame. Measurements were performed using a window size of 5.4 mm axially and 1.8 mm laterally, with 90% and 33% overlap, respectively. The axial and lateral displacement measurements were then spatially smoothed with a moving average filter (3×3) and accumulated in time to approximate the total displacement field.

The image registration algorithm was designed to measure to the total displacement field from the initial image frame to the final frame, with common reference coordinates. The optimization function used for this work, adapted from Richards and Doyley (2013), was:

$$\pi[\mathrm{u}(\mathrm{x})] = \sum_{i-1}^{N-1} \int_{\Omega} \frac{1}{2} \left(I_i(x+\mathbf{u}_i(\mathbf{x})) - I_{i+1}\left(x+\mathbf{u}_{i+1}(\mathrm{x})\right)\right)^2 + \frac{\alpha}{2}\left(\nabla\left(\mathbf{u}_{i+\mathbf{1}}-\mathbf{u}_i\right)^{sym} : \nabla\left(\mathbf{u}_{i+\mathbf{1}}-\mathbf{u}_i\right)^{sym}\right) d\Omega \quad (1)$$

Here, $I_i(\mathbf{x})$ was the ith frame of the 2D ultrasound image sequence and $\mathbf{u}_i(\mathbf{x})$ was the ith displacement measurement in two dimensions. All displacement fields share a common reference coordinate system, $\mathbf{x}$, with the initial image frame (i.e. $\mathbf{u}_1(\mathbf{x})=\mathbf{0}$). Subsequent image frames are non-linearly warped by the current guess of the displacement measurement. The first term in the above equation is a least squares matching of the ith image frame to each subsequent (ith $+1$) frame. The second term is a regularization of the incremental, frame-to-frame strain tensor fields, which is calculated as the symmetric part of the displacement gradient ($\varepsilon=\nabla\mathbf{u}^{sym}=(\nabla\mathbf{u}+\nabla\mathbf{u}^{\mathrm{T}})/2$). The regularization parameter, α, was empirically set to 2e11 for all measurements. For analysis, the total strain tensor field is calculated from the total displacement field ($\varepsilon_N=\nabla\mathbf{u}_N{}^{sym}$). The maximum and minimum principal strain components are found by calculating the eigenvalues of the total strain fields. Compressive strain was defined as the minimum principal strain, therefore a larger negative number indicated a greater compressive strain.

The region of tendon overlying the bursal prominence, defined as 1 cm of tendon distal to the most superior portion of the posterior calcaneus, was selected for analysis. It was then further subdivided into two equal height regions of interests: superficial and deep (Fig. 3a). The compressive strain at a 30 mm heel

Please cite this article as: Chimenti, R.L., et al., Ultrasound strain mapping of Achilles tendon compressive strain patterns during dorsiflexion. Journal of Biomechanics (2015), http://dx.doi.org/10.1016/j.jbiomech.2015.11.008

height was operationally defined as 0%. The tracking of tissue displacement superimposed on a b-mode ultrasound video concurrent with the tendon compressive strain during the combined heel lowering and partial squat task can be viewed with the electronic version of this manuscript.

2.4. Validity and reliability

The validity of the strain measurement algorithm was tested by simultaneously compressing a tissue mimicking phantom a known amount using a caliper and imaging with ultrasound. A 10% by mass polyvinyl alcohol (PVA), 0.2% silica and water solution was molded into a 1 cm height × 2 cm width × 4 cm length sample and cycled through several freeze-thaw combinations to form a phantom with ultrasound properties mimicking those of homogeneous soft tissue. A custom designed caliper attachment was 3D printed in plastic to hold the ultrasound transducer in line with the phantom. The US image was aligned axially with the phantom height (1 cm), laterally with the phantom length (4 cm) and positioned in a central location along the phantom width (Fig. 4a). Ultrasound image sequences were acquired while the tissue phantom was compressed from an initial width of 10 mm to a final compressed length (Fig. 4b). The initial and final compressive strain was measured directly via a caliper to the nearest 10 μm. Six image sequences were acquired during compressive strain with known caliper-imposed strain values ranging from 5 to 30%. Compressive strain was calculated in the same manner as the Achilles tendon estimates. A centrally located region of interest was isolated within the imaged phantom area with an approximate area of 8 mm axially and 28 mm laterally (Fig. 4b) and it was assumed that within this image region the measured strain should be approximately constant and equal to the caliper-imposed strain values. The Bland–Altman test was used to test the agreement between caliper imposed and ultrasound elastography measured strain estimates.

The effect of transducer motion relative to the skin on compressive strain was minimal compared to the magnitude of strain during dorsiflexion tasks. The ankle brace and transducer were positioned on a subject, and the probe was moved in several directions to approximate the maximum amount of probe motion within the brace. The transducer displacements, including elevational shifts (up and down) and lateral shifts (left and right), of 4 mm were measured with a digital caliper. In addition, just above the plastic shell component of the brace, the transducer was pushed 4 mm on each side resulting in a lateral tilt of the transducer. Each pair of data (up/down, left/right, tilt to left/right) was averaged to estimate the effect of each type of motion.

For test–retest reliability the heel lowering task was repeated four times in two subjects. The ankle brace and probe were removed and repositioned between each trial. The intraclass correlation coefficient for the superficial and deep regions of the tendon was examined.

2.5. Statistical analysis

Two-way repeated measures ANOVA was used to examine the effect of task (lowering from a heel lift, partial squat and a combination of both tasks in succession) and tendon region (superficial, deep). Pairwise comparisons with Bonferroni correction were used to compare the amount of tendon strain between tasks. Statistical significance was defined as a two-tailed P value ≤ 0.05.

3. Results

There was good agreement between the ultrasound elastography estimates and the caliper-induced strain. The values for the caliper-imposed strain (ε_{cal}) and the mean and standard deviation of the elastographic strain (ε_{us}) are shown in Fig. 4c. Ultrasound elastography underestimated the caliper-induced strain by 2.2% (95% confidence interval of the mean difference was 0.9–3.4%). The Bland–Altman test indicated that there was not a proportional bias in the difference between measures as a function of the average value of the measures ($P=0.332$). Motion of the transducer relative to the skin resulted in

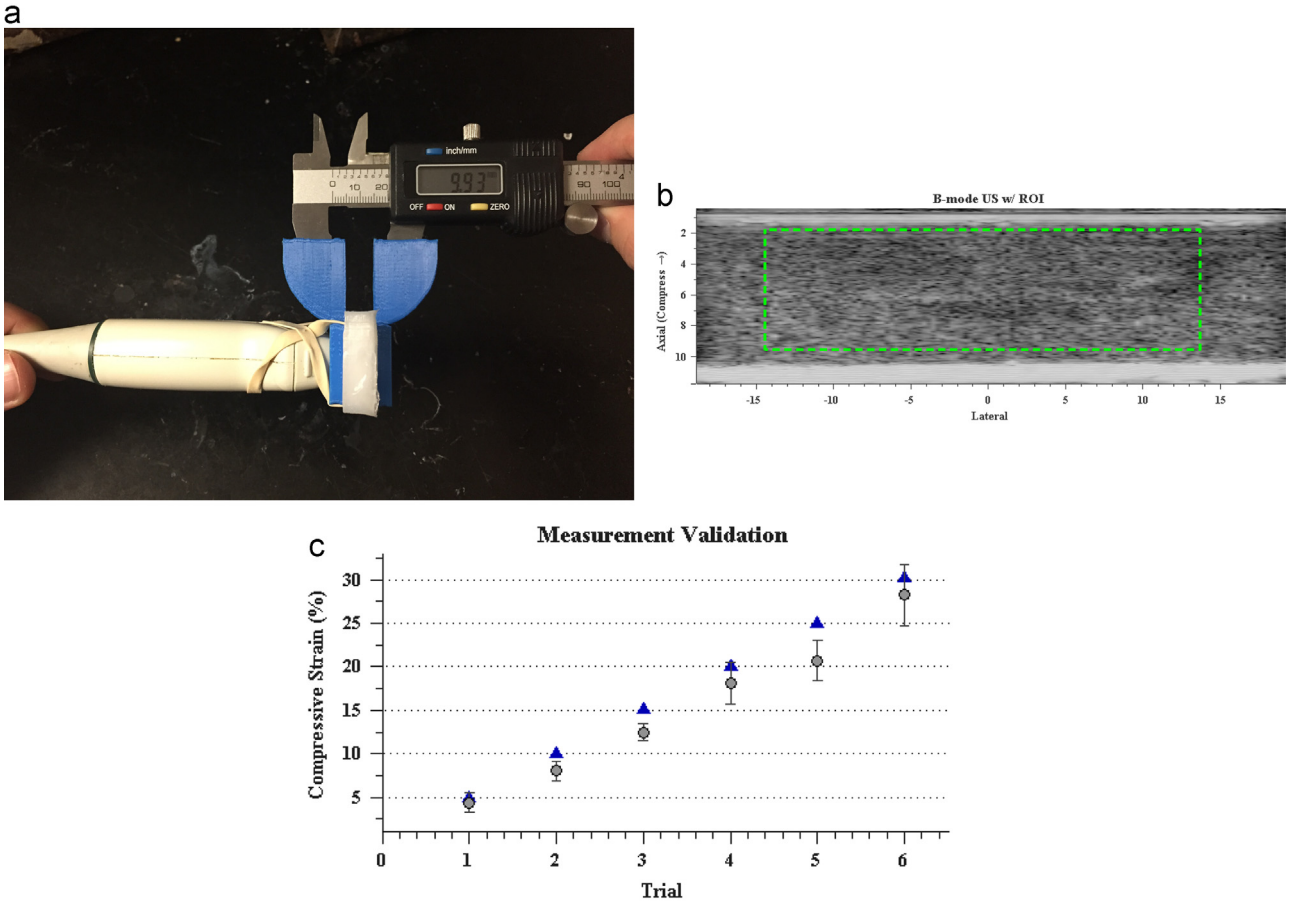

Fig. 4. (a) Ultrasound elastography validation setup and PVA tissue mimicking phantom. Caliper was used to control the magnitude of the phantom compression, (b) B-mode ultrasound image of tissue mimicking phantom with region of interest outlined in green and (c) caliper induced compressive strain (Δ) for 6 trials and their corresponding ultrasound elastography strain measurements (o) . (For interpretation of the references to color in this figure, the reader is referred to the web version of this article)..

Please cite this article as: Chimenti, R.L., et al., Ultrasound strain mapping of Achilles tendon compressive strain patterns during dorsiflexion. Journal of Biomechanics (2015), http://dx.doi.org/10.1016/j.jbiomech.2015.11.008

minimal error (<1%) of strain estimates (up/down: deep=−0.2%, superficial=−0.3%; left/right: deep=−0.5%, superficial=−0.8%; tilting: deep=−0.3%, superficial=−0.7%). The test–retest reliability was good for the deep (ICC=0.89, SEM=2.0%) and superficial (ICC=0.78, SEM=2.1%) regions of the tendon.

There was a main effect of task ($P<.001$) and tendon region ($P=.001$) on strain (Fig. 5). Pairwise comparisons demonstrated that there was greater compressive strain during the combined task of lowering and partial squat compared to lowering ($P=.001$) and a partial squat ($P<.001$). There was no statistical difference in tendon strain between the individual tasks of lowering and partial squat ($P=1.000$). There was significantly greater strain in the deep region (Lowering: $-12.2\pm6.0\%$, Partial squat: $-11.8\pm5.8\%$, Lowering and partial squat: $-20.7\pm8.1\%$) of the tendon compared to the superficial (Lowering: $-8.3\pm4.5\%$, Partial squat: $-7.4\pm4.2\%$, Lowering and partial squat: $-14.7\pm6.1\%$) for all tasks ($P=0.001$).

4. Discussion

This is the first study to report compressive strains in the Achilles tendon and show that the deep side of the tendon compresses more than the superficial region during dorsiflexion. Given that the deep side of the Achilles tendon insertion is often the primary site of pathology in patients with IAT, the findings of the current study highlight the potential need to reduce compressive strain of the tendon insertion in this population. Also, this is the first study to demonstrate that heel lifts reduce compressive strain of the Achilles tendon insertion in healthy adults. The development of a valid and reliable ultrasound elastography method to quantify compressive strain could be a useful tool to assess the effectiveness of interventions designed to alter compressive strain of the tendon insertion.

Advantages of using the non-rigid image registration based strain estimator used in the current study include its ability to accurately estimate *in vivo* tendon compressive strain with high reliability. The relatively low error (<1%) that occurred when the transducer was moved relative to a stationary tendon highlight the ability of the algorithm to track tissue specific landmarks relative to tissue in the same field of view. In addition this technique was able to reliably capture high magnitudes of strain *in vivo*. Yet the technique is not without limitations, strain decorrelation can still affect the measurement of tendon compressive strain. In our experience, there were three key factors that contributed to poor image similarity: (1) change in echogenicity with tendon strain (Duenwald et al., 2011), (2) occasional artifacts due to out of plane motion and (3) changes in the rate of tendon strain. The first two factors are inherent to examining the Achilles tendon *in vivo* with 2D imaging, and the third can be adjusted be altering the frequency of frames used for analysis. While initially a similar number of image frames were used for analysis for all subjects, there were a few trials in which we increased the number of frames to compensate for a large increase in strain rate. Despite these factors lowering image similarity, the algorithm was robust enough to detect consistent patterns of compressive strain within the Achilles tendon insertion.

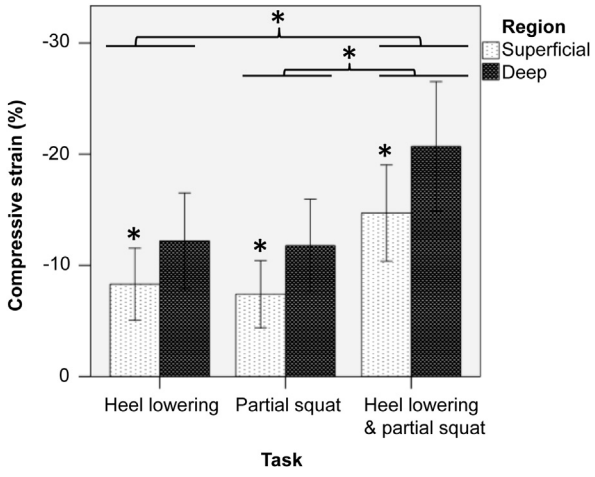

Fig. 5. Asterisks indicate significant differences in compressive strain between Achilles tendon regions and between tasks. Tendon compressive strain was quantified by the minimum principal strain during 3 tasks.

The first hypothesis of the study was supported by lower tendon compressive strain when performing a partial squat with a heel lift than without ($P<.001$). Both ankle dorsiflexion (Partial squat: $-11.8\pm5.8\%$) and lowering from a heel lift (Lowering: $-12.2\pm6.0\%$) resulted in compressive strain of the deep side of the Achilles tendon insertion. Yet the amount of compressive strain nearly doubled when both of these tasks were combined (Lowering and partial squat: $-20.7\pm8.1\%$). Based on these findings, tendon compressive strain can be minimized by either avoiding squatting activities, which require ankle dorsiflexion, or using heel lifts, which places the ankle into relative plantar flexion.

The second hypothesis was supported by greater compressive strain on the deep side of the tendon compared to the superficial region. This finding was consistent across all tasks and among all participants in the current study ($P=0.001$). The magnitude of compressive strain measured in the current study includes a decrease in tendon thickness that naturally occurs during tendon lengthening due to the Poisson effect (Vergari et al., 2011). The pattern of increased compressive strain at the location where patients with IAT typically have pathology, indicates that this area of the tendon insertion experiences greater compressive strain than would be expected due to tendon lengthening alone. Theoretically, repeated compressive strain of the Achilles tendon during daily activities could lead to adaptation and/or pathology of the tissue. Further research is needed to understand how pathology affects the pattern of compressive strain within the tendon.

A limitation of the methods in the current study was achieving a state of zero compressive strain for the Achilles tendon. Ideally, there would be no forces on the Achilles tendon in the reference position for each task, such as sitting with the ankle plantar flexed. However, in pilot work it was difficult to maintain the region of interest within the transducer's field of view during the transition from non-weight-bearing to weight-bearing. To reduce superior–inferior motion yet still achieve a low stress state, a weight-bearing reference position of standing with the ankle plantar flexed was used. A heel lift height of 30 mm, or inclination of 17°, was chosen since it is toward the upper end of what we considered feasible to wear as a shoe insert. Thus, although the current study was unable to quantify the amount of tendon compressive strain relative to a true zero stress state, measurements were successfully performed with a low-stress reference position. Another limitation is that the heel lift height of 30 mm is greater than that prescribed in common clinical practice. A standard heel lift given to IAT patients is typically 12–15 mm thick, however this height is not chosen based on clinical evidence of efficacy. Further research is needed to determine if lower heel lift heights are effective at reducing tendon compressive strain.

5. Conclusions

This is the first study to report that the area of the tendon insertion often involved in IAT pathology experiences greater compressive strain than more superficial regions during dorsiflexion. This finding implicates a potential role of compressive strain in the development and progression of IAT. This is also the first study to demonstrate that a heel lift reduces compressive strain of the Achilles tendon insertion in healthy adults. Before clinical recommendations can be made, research is needed in patients with Achilles tendinopathy.

Please cite this article as: Chimenti, R.L., et al., Ultrasound strain mapping of Achilles tendon compressive strain patterns during dorsiflexion. Journal of Biomechanics (2015), http://dx.doi.org/10.1016/j.jbiomech.2015.11.008

Conflicts of interest statement

The authors have no conflicts of interest regarding the present study.

Acknowledgments

We gratefully acknowledge the support of NIH R03 AR06748401 and the University of Rochester Core Center for Musculoskeletal Biology and Medicine.

Appendix A. Supplementary material

Supplementary data associated with this article can be found in the online version at http://dx.doi.org/10.1016/j.jbiomech.2015.11.008.

References

Akizuki, K.H., Gartman, E.J., Nisonson, B., Ben-Avi, S., McHugh, M.P., 2001. The relative stress on the Achilles tendon during ambulation in an ankle immobiliser: implications for rehabilitation after Achilles tendon repair. Br. J. Sport. Med. 35 (5), 329–333, discussion 333-324.

Andriacchi, T.P., Andersson, G.B., Fermier, R.W., Stern, D., Galante, J.O., 1980. A study of lower-limb mechanics during stair-climbing. J. Bone Jt. Surg .Am. 62 (5), 749–757.

Athanasiou, A., Tardivon, A., Tanter, M., Sigal-Zafrani, B., Bercoff, J., Deffieux, T., … Neuenschwander, S., 2010. Breast lesions: quantitative elastography with supersonic shear imaging–preliminary results. Radiology 256 (1), 297–303. http://dx.doi.org/10.1148/radiol.10090385.

Brown, P.G., Alsousou, J., Cooper, A., Thompson, M.S., Noble, J.A., 2013. The AutoQual ultrasound elastography method for quantitative assessment of lateral strain in post-rupture Achilles tendons. J. Biomech. 46 (15), 2695–2700. http://dx.doi.org/10.1016/j.jbiomech.2013.07.044.

Carcia, C.R., Martin, R.L., Houck, J., Wukich, D.K., Orthopaedic Section of the American Physical Therapy, A., 2010. Achilles pain, stiffness, and muscle power deficits: achilles tendinitis. J. Orthop. Sport. Phys. Ther. 40 (9), A1–26. http://dx.doi.org/10.2519/jospt.2010.0305.

Cespedes, I.I., M., Ophir, J., 1997. Theoretical bounds on strain estimation in elastography. Ultrasonics, Ferroelectr. Freq. Control IEEE Trans. 44 (1), 164–172.

Duenwald, S., Kobayashi, H., Frisch, K., Lakes, R., Vanderby Jr., R., 2011. Ultrasound echo is related to stress and strain in tendon. J. Biomech. 44 (3), 424–429. http://dx.doi.org/10.1016/j.jbiomech.2010.09.033.

Farris, D.J., Buckeridge, E., Trewartha, G., McGuigan, M.P., 2012. The effects of orthotic heel lifts on Achilles tendon force and strain during running. J. Appl. Biomech. 28 (5), 511–519.

Farron, J., Varghese, T., Thelen, D.G., 2009. Measurement of tendon strain during muscle twitch contractions using ultrasound elastography. IEEE Trans. Ultrason. Ferroelectr. Freq. Control 56 (1), 27–35. http://dx.doi.org/10.1109/TUFFC.2009.1002.

Franz, J.R., Slane, L.C., Rasske, K., Thelen, D.G., 2015. Non-uniform in vivo deformations of the human Achilles tendon during walking. Gait Posture 41 (1), 192–197. http://dx.doi.org/10.1016/j.gaitpost.2014.10.001.

Gennisson, J.L., Deffieux, T., Mace, E., Montaldo, G., Fink, M., Tanter, M., 2010. Viscoelastic and anisotropic mechanical properties of in vivo muscle tissue assessed by supersonic shear imaging. Ultrasound Med. Biol. 36 (5), 789–801. http://dx.doi.org/10.1016/j.ultrasmedbio.2010.02.013.

Johanson, M.A., Allen, J.C., Matsumoto, M., Ueda, Y., Wilcher, K.M., 2010. Effect of heel lifts on plantarflexor and dorsiflexor activity during gait. Foot Ankle Int. 31 (11), 1014–1020. http://dx.doi.org/10.3113/FAI.2010.1014.

Kallel, F., Varghese, T., Ophir, J., Bilgen, M., 1997. The nonstationary strain filter in elastography: Part II. Lateral and elevational decorrelation. Ultrasound Med. Biol. 23 (9), 1357–1369.

Karjalainen, P.T., Soila, K., Aronen, H.J., Pihlajamaki, H.K., Tynninen, O., Paavonen, T., Tirman, P.F., 2000. MR imaging of overuse injuries of the Achilles tendon. Am. J. Roentgenol. 175 (1), 251–260.

Kim, Y.S., Kim, J.M., Bigliani, L.U., Kim, H.J., Jung, H.W., 2011. In vivo strain analysis of the intact supraspinatus tendon by ultrasound speckles tracking imaging. J. Orthop. Res. 29 (12), 1931–1937. http://dx.doi.org/10.1002/jor.21470.

Korstanje, J.W., Scheltens-De Boer, M., Blok, J.H., Amadio, P.C., Hovius, S.E., Stam, H. J., Selles, R.W., 2012. Ultrasonographic assessment of longitudinal median nerve and hand flexor tendon dynamics in carpal tunnel syndrome. Muscle Nerve 45 (5), 721–729. http://dx.doi.org/10.1002/mus.23246.

Kujala, U.M., Sarna, S., Kaprio, J., 2005. Cumulative incidence of achilles tendon rupture and tendinopathy in male former elite athletes. Clin. J. sport Med.: Off. J. Can. Acad. Sport Med. 15 (3), 133–135.

Lee, K.H., Shieh, J.C., Matteliano, A., Smiehorowski, T., 1990. Electromyographic changes of leg muscles with heel lifts in women: therapeutic implications. Arch. Phys. Med. Rehabil. 71 (1), 31–33.

Leitze, Z., Sella, E.J., Aversa, J.M., 2003. Endoscopic decompression of the retrocalcaneal space. J. Bone Jt. Surg. (Am. Vol.) 85-A (8), 1488–1496.

Lichtwark, G.A., Wilson, A.M., 2006. Interactions between the human gastrocnemius muscle and the Achilles tendon during incline, level and decline locomotion. J. Exp. Biol. 209 (21), 4379–4388. http://dx.doi.org/10.1242/jeb.02434.

Lopata, R.G., Nillesen, M.M., Hansen, H.H., Gerrits, I.H., Thijssen, J.M., de Korte, C.L., 2009. Performance evaluation of methods for two-dimensional displacement and strain estimation using ultrasound radio frequency data. Ultrasound Med. Biol. 35 (5), 796–812. http://dx.doi.org/10.1016/j.ultrasmedbio.2008.11.002.

Lopata, R.G., van Dijk, J.P., Pillen, S., Nillesen, M.M., Maas, H., Thijssen, J.M., … de Korte, C.L., 2010. Dynamic imaging of skeletal muscle contraction in three orthogonal directions. J. Appl. Physiol. (1985) 109 (3), 906–915. http://dx.doi.org/10.1152/japplphysiol.00092.2010.

Muller, M., Gennisson, J.L., Deffieux, T., Tanter, M., Fink, M., 2009. Quantitative viscoelasticity mapping of human liver using supersonic shear imaging: preliminary in vivo feasibility study. Ultrasound Med. Biol. 35 (2), 219–229. http://dx.doi.org/10.1016/j.ultrasmedbio.2008.08.018.

Nester, C.J., Jarvis, H.L., Jones, R.K., Bowden, P.D., Liu, A., 2014. Movement of the human foot in 100 pain free individuals aged 18-45: implications for understanding normal foot function. J. Foot Ankle Res. 7 (1), 51. http://dx.doi.org/10.1186/s13047-014-0051-8.

Ophir, J., Cespedes, I., Ponnekanti, H., Yazdi, Y., Li, X., 1991. Elastography: a quantitative method for imaging the elasticity of biological tissues. Ultrason. Imaging 13 (2), 111–134.

Richards, M.S., Barbone, P.E., Oberai, A.A., 2009. Quantitative three-dimensional elasticity imaging from quasi-static deformation: a phantom study. Phys. Med. Biol. 54 (3), 757–779. http://dx.doi.org/10.1088/0031-9155/54/3/019.

Richards, M.S., Doyley, M.M., 2013. Non-rigid image registration based strain estimator for intravascular ultrasound elastography. Ultrasound Med. Biol. 39 (3), 515–533. http://dx.doi.org/10.1016/j.ultrasmedbio.2012.09.023.

Scott, L.A., Munteanu, S.E., Menz, H.B., 2015. Effectiveness of orthotic devices in the treatment of achilles tendinopathy: a systematic review. Sport. Med. 45 (1), 95–110. http://dx.doi.org/10.1007/s40279-014-0237-z.

Shibuya, N., Thorud, J.C., Agarwal, M.R., Jupiter, D.C., 2012. Is calcaneal inclination higher in patients with insertional Achilles tendinosis? A case-controlled, cross-sectional study. J. Foot Ankle Surg. 51 (6), 757–761. http://dx.doi.org/10.1053/j.jfas.2012.06.015.

Slane, L.C., Thelen, D.G., 2015. Achilles tendon displacement patterns during passive stretch and eccentric loading are altered in middle-aged adults. Med. Eng. Phys. 37 (7), 712–716. http://dx.doi.org/10.1016/j.medengphy.2015.04.004.

Varghese, T.O., J., 1997. A theoretical framework for performance characterization of elastography: the strain filter. Ultrason. Ferroelectr. Freq. Control IEEE Trans. 44.1, 164–172.

Vergari, C., Pourcelot, P., Holden, L., Ravary-Plumioen, B., Gerard, G., Laugier, P., Crevier-Denoix, N., 2011. True stress and Poisson's ratio of tendons during loading. J. Biomech. 44 (4), 719–724. http://dx.doi.org/10.1016/j.jbiomech.2010.10.038.

Yoshii, Y., Henderson, J., Villarraga, H.R., Zhao, C., An, K.N., Amadio, P.C., 2011. Ultrasound assessment of the motion patterns of human flexor digitorum superficialis and profundus tendons with speckle tracking. J. Orthop. Res. 29 (10), 1465–1469. http://dx.doi.org/10.1002/jor.21428.

Please cite this article as: Chimenti, R.L., et al., Ultrasound strain mapping of Achilles tendon compressive strain patterns during dorsiflexion. Journal of Biomechanics (2015), http://dx.doi.org/10.1016/j.jbiomech.2015.11.008